Stopping Powers and Inelastic Mean Free Path of 100 eV to 30 keV Electrons in Zirconium Silicates

D. Tahir[*], Suarga, Yulianti and N.H. Sari

Department of Physics, Faculty of Mathematics and Natural Sciences, Hasanuddin University
Jl. Perintis Kemerdekaan Km 10, Makassar 90245, Indonesia

A R T I C L E   I N F O

A B S T R A C T

We have determined the electron stopping power (SP) and inelastic mean free path (IMFP) of $(ZrO_2)_x(SiO_2)_{1-x}$ (x=1, 0.75, 0.5, 0.25, 0) for electron energies from 100 eV to 30 keV by means of modified Born–Ochkur equations. The energy loss function (ELF) is required in the calculation of SP and IMFP. We used the electron energy losses from 0 to 80 eV obtained by quantitative analysis of reflection electron energy-loss spectroscopy (REELS) spectra. The values of SP and IMFP for high contents of ZrO_2 (x=50% and x=75%) in Zr-silicates are similar to those of ZrO_2, and similar to those of SiO_2 for low contents of ZrO_2 (x=25%) in Zr-silicates. There are small differences in the values of SP and IMFP for ZrO_2 and SiO_2. We found that the SP decreases while the IMFP increases with increasing electron energy. We have demonstrated that the ELF obtained from the quantitative analysis of REELS spectra provide us with a straightforward way to determine SP and IMFP for alloy materials by using modified Born-Ochkur equations.

INTRODUCTION

Zirconium oxide and zirconium silicates have received great attention and exhibit important nuclear applications as engineering materials for inert matrix fuels, actinide waste forms and targets for transmutation of radionuclides, due to its high chemical durability, high corrosion resistance, low hydrogen absorption, and excellent radiation stability [1-5].

The development of new zirconium oxides for use as radiation tolerant materials in advanced nuclear energy systems has resulted in materials with unique physical and chemical properties. Many experimental studies have reported on the effects of crack growth [4], high pressure steam [1], and irradiation of heavy ions [3], He nuclei [3], and protons [2] on the electronic, chemical, and structural properties of zirconium oxide. However, we found few studies devoted to the electron stopping power (SP) and inelastic mean free path (IMFP) properties of zirconium oxide and zirconium silicates for a wide range of energy loss functions (ELFs) up to 80 eV.

The electron SP and IMFP properties describe the traverses of energetic electron through matter under interactions with atomic orbital electrons and atomic nuclei. Through these interactions, the electrons may lose their kinetic energy through elastic or inelastic collisions. In an elastic collision the electron is deflected from its original path but no energy loss occurs, while in an inelastic collision the electron is deflected from its original path and part of its energy is transferred to an orbital electron or emitted in the form of bremsstrahlung production. Electrons lose their kinetic energy through various types of inelastic scattering processes described by SP, while the mean distance between two collisions is described by the IMFP [6-12]. These two fundamental quantities are essential importance in many fields of research, such as radiobiology, biomedical applications, radiation dosimetry, and the modeling of electron transport in matter for many other applications. For instance, to understand radiation effects in radiation dosimetry, SP values are required for the calculation of energy deposition of energetic electrons passing through biological tissues [6-9]. SP values have also been used in Monte Carlo simulations of electron transport relevant to electron-probe microanalysis, Auger-electron spectroscopy, and dimensional metrology in the scanning electron microscope [10-12].

In this study, we report electron SP and IMFP values calculated from the energy loss function (ELF) of zirconium oxide, silicon dioxide, and zirconium silicates for energies from 100 eV to 30 keV. The ELFs are obtained from the experimental reflection electron energy loss

---

[*] Corresponding author.
   E-mail address: allanctahir@yahoo.com

spectroscopy (REELS) spectra. REELS is surface sensitive and the spectra carries information on the electronic structure of the material because the energy loss experienced by the incident electron depends on the electronic structure of the material. The spectra can easily be recorded over a wide energy-loss range [13-29]. The calculation of the ELFs of zirconium oxide, silicon dioxide, and zirconium silicates from REELS spectra has already been performed by Tahir *et. al.* [15]. Subsequently, the calculated SPs were compared with the results of evaluating the nonrelativistic Bethe equation, while the IMFPs were compared with the results of Tanuma Powell Penn (TPP-2M) methods [9] and Ashley *et. al.* [30], which are available from a National Institute of Standards and Technology (NIST) database. The aim of this work are twofold, namely: first, to provide an alternative basic data of SPs and IMFPs for the study on the energy deposition of low-energy electrons transport through zirconium oxide and zirconium silicates; and second, to show that the method presented in this study might be a good one for evaluating the SP and IMFP of radiation tolerant materials in advanced nuclear energy applications.

EXPERIMENTAL METHOD

According to the dielectric response theory, the Penn statistical approximation, and the Born–Ochkur correction method which includes the exchange effect between the incident electron and the electrons in the medium, the electron inelastic differential cross section can be expressed as [7]:

$$\frac{d^2\sigma}{d(\hbar\omega)dq} = \frac{1}{\pi a_0 E} \int_0^\infty \frac{\omega'}{\omega} \frac{1}{q} \mathrm{Im}[-1/\varepsilon(\omega')]$$

$$\mathrm{x}\; \delta\left(\omega - \omega' - \frac{\hbar q^2}{2m}\right) C_{ex} d\omega' \quad (1a)$$

where

$$C_{ex} = 1 - \frac{Q}{E + \hbar\omega' - \hbar\omega} + \left(\frac{Q}{E + \hbar\omega' - \hbar\omega}\right)^2 \;,\; \text{and}$$

$$Q = \hbar^2 q^2 / 2m \quad (1b)$$

With Eq. (1) and over all allowed integration region, the SP and IMFP can be given as follows [7-9]:

$$SP = -\frac{dE}{dS} = \frac{1}{2\pi a_0 E} \int_0^{E/2} (\hbar\omega) \mathrm{Im}[-1/\varepsilon(\omega)] v(\alpha) d(\hbar\omega) \quad (2)$$

$$\lambda = \left(\frac{1}{2\pi a_0 E} \int_0^{E/2} \mathrm{Im}[-1/\varepsilon(\omega)] w(\alpha) d(\hbar\omega)\right)^{-1} \quad (3)$$

Where E is the kinetic energy of the incident electron, α_0 is the Bohr radius, $\hbar\omega$ is the energy loss, $\mathrm{Im}[-1/\varepsilon(\omega)]$ is the energy loss function, $v(\alpha)$ and $w(\alpha)$ are, respectively:

$$v(\alpha) = \frac{2s}{(1+\alpha)(1+\alpha+s)} + \ln\left\{\frac{(1-\alpha^2)(1+\alpha)}{(1-\alpha-s)(1+\alpha+s)^2}\right\} \quad (4)$$

$$w(\alpha) = \frac{3\alpha^2 + 3\alpha + 1}{(1+\alpha)^2} \ln\frac{1+\alpha-s}{1+\alpha} + \ln\frac{1-\alpha}{1-\alpha-s}$$

$$+ \frac{2\alpha^2 + \alpha}{(1+\alpha)^2} \ln\frac{1+\alpha}{1+\alpha+s} + \frac{2\alpha s}{(1+\alpha)^2(1+\alpha+s)} \quad (5)$$

With $\alpha = \hbar\omega / E$ and $S = \sqrt{1-2\alpha}$

Tan *et. al.* [7] used the Born-Ochkur exchange correction in the calculation of SPs and IMFPs of organic compound. The results of their calculations of SPs attain similar accuracy with Ashley exchange correction for all electron energy region and also agree well with Bethe-Bloch theory at high-energy region.

As shown by equation (2) and (3), the calculations of SP and IMFP require the energy loss function (ELF), which completely determines the probability of an inelastic scattering event, the energy loss, and the scattering angular distribution. The key problem for the calculation of SP and IMFP is deriving the ELF. The well-known Lindhard dielectric function is only applicable for a limited class of materials, namely the so called nearly-free electron materials such as Al or alkali metals, and is not valid for other materials such as noble metals, insulators, or organic compounds. On the other hand, the ELF in the long wave-length limit $k \rightarrow 0$ approaches the optical ELF, and is calculated from experimental optical data, the refractive index and the extinction coefficients, which are available for a number of materials [7-9].

Tahir *et. al.* [13,16,18,20-25] have employed the semi-classical dielectric response model proposed by Tougaard and Yubero [26-29] in their calculation of ELF. The algorithms of this method have been implemented in the generally available QUEELS-$\varepsilon(k,\omega)$-REELS software package [29]. The validity and consistency of this method was extensively tested recently [21] and it has also previously been successfully used to obtain the ELFs and optical properties of ultrathin dielectric [15,16,18] semiconductor [17], polymer [22], metals [14,23], and transparent oxide films [20,21,24,25]. In Ref. [14] there is a detailed discussion of

experimental tests of the validity of the elastic scattering model.

In this model, the dielectric function $\varepsilon(k,\omega)$ of the material describes all excitations. The dielectric function is a function of wave vector k and frequency ω which are the only inputs for the calculations in this model. The dielectric function is given in term of the energy loss function (ELF) Im($-1/\varepsilon$) which is parameterized as a sum of Drude-Lindhard type oscillators, as described in Refs. [14, 15, 27-29]:

$$\text{Im}\left\{\frac{-1}{\varepsilon(k,\omega)}\right\} = \theta(\hbar\omega - E_g)\sum \frac{A_i\gamma_i\hbar\omega}{\left(\hbar^2\omega_{0ik}^2 - \hbar^2\omega^2\right)^2 + \gamma_i^2\hbar^2\omega^2} , \quad (6)$$

where the dispersion relation is given in the form

$$\hbar\omega_{0ik} = \hbar\omega_{0i} + \alpha_i\frac{\hbar^2k^2}{2m} . \quad (7)$$

Here, A_i, γ_i, $\hbar\omega_{0i}$, and α_i are the oscillator strength, damping coefficient, excitation energy and momentum dispersion coefficient of the ith oscillator, respectively, and $\hbar k$ is the momentum transferred from the REELS electron to the solid. The dependence of ω_{0ik} on k is generally unknown, but we use Eq. (6) with α_i as an adjustable parameter. The values of the momentum dispersion coefficient α_i are related to the effective mass, e.g, $\alpha_i \approx 0$ for insulator and $\alpha_i \approx 1$ for metals [14,27-29]. The step function $\theta(\hbar\omega - E_g)$ is included to describe the effect of the band gap energy E_g in semiconductors and insulators. Here, $\theta(\hbar\omega - E_g)=0$ if $\hbar\omega < E_g$ and $\theta(\hbar\omega - E_g)=1$ if $\hbar\omega > E_g$. The band gap was estimated from the onset value of REELS spectrum as shown in Fig. 1 [15].
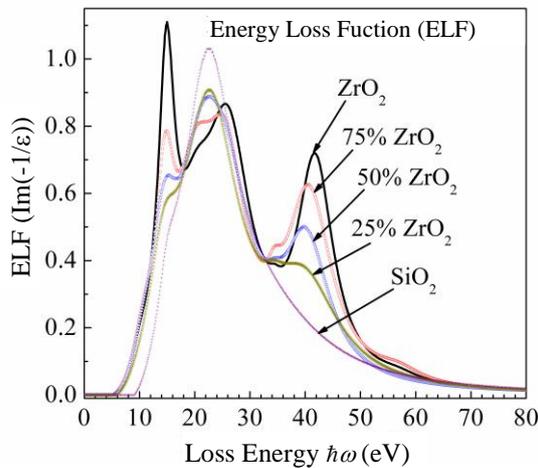
Fig. 1. Energy loss functions (ELFs) of ZrO$_2$, SiO$_2$, and (ZrO$_2$)$_x$(SiO$_2$)$_{1-x}$ from [15].

For materials studied in this work, we used data for ELF from Ref. [15] in which the parameters are obtained by fitting the inelastic electron scattering cross section $\lambda K_{th}(\hbar\omega)$ spectrum simulated with the QUEELS-$\varepsilon(k,\omega)$-REELS software to an experimental inelastic scattering cross section $\lambda K_{exp}(\hbar\omega)$. The parameters A_i, γ_i, $\hbar\omega_i$, and α_i, of the oscillators are varied until a good agreement between the calculated and experimental inelastic cross sections is obtained. The oscillator strengths are adjusted to make sure that $\varepsilon(k,\omega)$ fulfills the well-established Kramers-Kronig sum rule [14,27-29],

$$\frac{2}{\pi}\int_0^\infty \text{Im}\left\{\frac{1}{\varepsilon(k,\omega)}\right\}\frac{d(\hbar\omega)}{\hbar\omega} = 1 - \left(\frac{1}{n_0^2}\right) \quad (8)$$

Here, n_0 is the refractive index of the materials in the optical limit $\hbar\omega \rightarrow 0$. These parameters are listed in Table 1 in Ref. [15] for all considered materials.

Table 1. Stopping power (SP) and inelastic mean free path (IMFP) for SiO$_2$ and ZrO$_2$ as determined in this study.

E (eV)	SiO$_2$ SP	ZrO$_2$ SP	SiO$_2$ IMFP	ZrO$_2$ IMFP
100	3.1164	2.603	8.95	9.231
200	3.1207	2.8568	11.2038	12.2565
300	2.6053	2.517	14.0763	15.5254
400	2.2206	2.123	16.9597	18.0734
500	1.9381	1.8557	19.7855	20.2886
600	1.7236	1.7026	22.5499	22.5639
700	1.5553	1.5701	25.2584	24.8435
800	1.4195	1.4565	27.9179	27.1086
900	1.3076	1.3587	30.5334	29.3524
1000	1.2135	1.274	33.1107	31.5729
1500	0.9024	0.9784	45.5415	42.3425
2000	0.726	0.8013	57.418	52.6567
3000	0.5301	0.5969	80.0941	72.3337
4000	0.422	0.4808	101.8031	91.132
5000	0.3527	0.4051	122.8389	109.3111
6000	0.3042	0.3514	143.3645	127.019
7000	0.2682	0.3113	163.4829	144.3502
8000	0.2403	0.28	183.2643	161.3696
9000	0.218	0.2548	202.7597	178.1243
10000	0.1998	0.2341	222.0075	194.65
15000	0.1423	0.1683	315.397	274.6469
16500	0.1313	0.1556	342.6885	297.9771
18000	0.122	0.1449	369.7128	321.0614
19500	0.114	0.1356	396.4967	343.9247
21000	0.107	0.1275	423.0624	366.5873
22500	0.1009	0.1204	449.4284	389.0667
24000	0.0955	0.1141	475.6107	411.3776
25500	0.0907	0.1084	501.6231	433.5327
27000	0.0864	0.1034	527.4774	455.5431
28500	0.0825	0.0988	553.1842	477.4184
30000	0.0789	0.0946	578.7527	499.1671

RESULTS AND DISCUSSION

The SPs and IMFPs of zirconium oxide, silicon dioxide, and zirconium silicates have been

determined by using the ELFs obtained from quantitative analysis of REELS spectra. These ELFs were already obtained in the past by Tahir et.al. and explained in detail in Ref.[15]. The ELFs of ZrO_2, SiO_2, and Zr-silicates in Ref. [15] have been compared with experimental optical data and the method was validitated. Further, the method was successfully employed to obtain the ELFs of ultrathin dielectrics, semiconductors, polymers, metals, and transparent oxide films [14-25].

Figure 1 shows the ELFs of $(ZrO_2)_x(SiO_2)_{1-x}$ (x=1, 0.75, 0.5, 0.25, 0) from Refs. 15. These ELFs were determined from quantitative analysis of REELS data with primary energies of 0.5, 1.0, 1.5, and 2.0 keV. We now use the ELFs (Fig. 1) from Ref. [15] for calculation of the SPs and the IMFPs based on equation (2) and (3), respectively. Band gap values are indicated by the flat line in the low loss energy region of the ELFs in Fig. 1. The band gap values are 5.30, 5.35, 5.55, 5.95, and 9.0 eV for ZrO_2, $(ZrO_2)_{0.75}(SiO_2)_{0.25}$, $(ZrO_2)_{0.5}(SiO_2)_{0.5}$, $(ZrO_2)_{0.25}(SiO_2)_{0.75}$, and (SiO_2), respectively. The detail about band gap of Zr-silicates can be found elsewhere [13,15]. For ZrO_2, the main plasmon peaks appear around 15, 26, and 42 eV. The intensity of these plasmon peaks change as the contents of ZrO_2 changed in Zr-silicates. As can be seen in the Fig. 1, the plasmon peaks at 15 eV and 42 eV decreases, while the plasmon peak at 26 eV increases with decreasing ZrO_2 contents in Zr-silicates.

Figure 2 shows the SP and the IMFP of electron in ZrO_2 and SiO_2 for energies from 100 eV to 30 keV. In Fig. 2, we compare our results for ZrO_2 and SiO_2 to the SPs determined from the nonrelativistic Bethe equation for solid [9] and to the IMFPs determined using Tanuma Powell Penn (TPP-2M) formula. We also compare our IMFP results for SiO_2 with Ashley *et. al*. [30] which incorporates the exchange correction in their calculation but unfortunately there is no reference data for ZrO_2. The SP values for SiO_2 show good agreement with the predictions of nonrelativistic Bethe-theory; however, our SP for ZrO_2 is about 10% lower. The nonrelativistic Bethe-theory obtains the SPs without considering the exchange correction and gives accurate value at energies higher than 10 keV. The TPP-2M results for IMFP without exchange correction also shown in Fig. 2 for comparison. The IMFP values for SiO_2 show good agreement with TPP-2M and Ashley, while for ZrO_2 our IMFP values are about 25% larger than those obtained from TPP-2M. The calculation of IMFP by using TPP-2M ignored the effect of surface elastic scattering and interference between surface and bulk excitation [9,15].

The ELFs used in this study are obtained from the experimental reflection electron energy loss spectroscopy (REELS) spectra which includes all effects of interactions between incident electron and electron in matter [15].
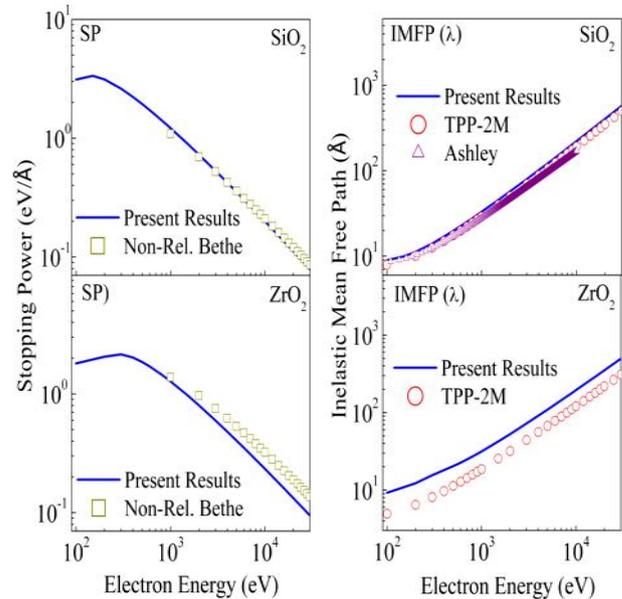
Fig. 2. Comparison of stopping power (SP) and inelastic mean free path (IMFP) of SiO_2 and ZrO_2 obtained in this study (line) with available theoretical data. The SP is compared with the results of nonrelativistic Bethe equation (symbol (□)) and the IMFP is compared with the results of TPP-2M (symbol (O)) [9]. For SiO_2 the IMFP from Ashley *et. al*. (symbol (Δ)) was included [30].

Figure 3 shows the SP and IMFP values for Zr-silicates for various electrons energies. For high contents of ZrO_2 (x=50% and x=75%) in Zr-silicates, the SP and IMFP values are similar to those of ZrO_2; however, or a low content of ZrO_2 (x=25%) in Zr-silicates, they are similar to those of SiO_2. As can be seen in Table 1 and Fig. 3, the value of SP and IMFP calculated in this study for ZrO_2 and SiO_2 are similar. The similarity of those values is due to the similarity of the universal inelastic electron cross sections for the oxide materials [27]. The SP decreases while the IMFP increases with increasing electron energy. For estimating SP and IMFP, based on the simple nonrelativistic Bethe and TPP-2M formula, respectively, we need material parameters such as bulk density, number of valence electrons per molecule, mean excitation energy, and energy band gap values. For alloys, some of these parameters are difficult to directly find from the handbooks. However, even in such a case, equations 2 and 3 enable us to easily calculate the SPs and IMFPs of Zr-silicates from the quantitative analysis of REELS spectra.
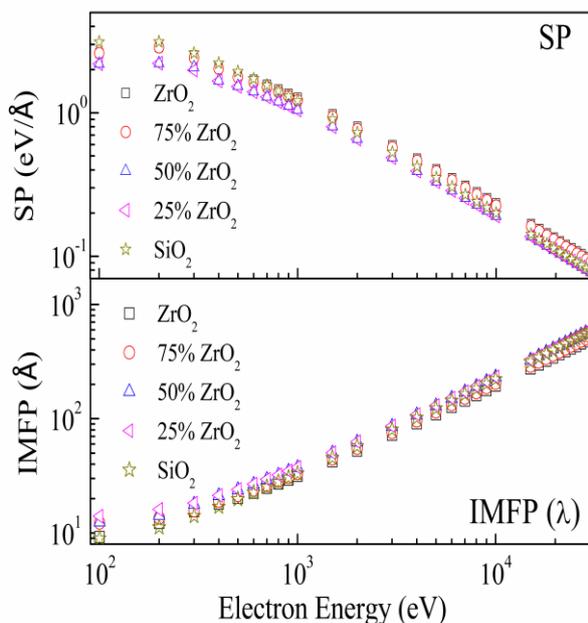
Fig. 3. The stopping power (SP) and the inelastic mean free path (IMFP) of $(ZrO_2)_x(SiO_2)_{1-x}$ (x=0, 0.25, 0.50, 0.75, and 1.0) in this study as calculated by using the equation (2) and (3) from ELF determined from quantitative analysis of REELS spectra.

CONCLUSION

The SPs and IMFPs of Zr-silicates have been obtained for electron energies from 100 eV to 30 keV by using ELF from the quantitative analysis of REELS spectra in the modified Born–Ochkur equations. The values of SP and IMFP indicate that the ZrO_2 has a strong effect on the electronic properties of Zr-silicates for ZrO_2 contents of 50% and 75% in the silicates. However, for the ZrO_2 content of 25%, the SiO_2 has a strong effect on electronic properties of Zr-silicates. In summary, we have demonstrated that the applied procedure for using the ELF obtained from quantitative analysis of REELS spectra provides us with a straightforward means to determine the SPs and IMFPs of alloys for electron energies from 100 eV to 30 keV.

REFERENCES

1. K. Park, S. Yang and K. Ho, J. Nucl. Mater. **420** (2012) 39.

2. K. Une, I. Takagi, K. Sawada, H. Watanabe, K. Sakamoto and M. Aomi, J. Nucl. Mater. **420** (2012) 445.

3. F. Lu, J. Wang, M. Lang, M. Toulemonde, F. Namavar, C. Trautmann, J. Zhang, R. C. Ewing and J. Lian, J. Phys. Chem. **14** (2012) 12295.

4. P.A. Raynaud, D.A. Koss and A.T. Motta, J. Nucl. Mater. **420** (2012) 69.

5. T. Yang, X. Huang, Y. Gao, C. Wang, Y. Zhang, J. Xue, S. Yan and Y. Wang, J. Nucl. Mater. **420** (2012) 430.

6. M. Behar, C.D. Denton, R.C. Fadanelli, I. Abril, E.D. Cantero, R.G. Molina and L.C.C. Nagamine, Eur. Phys. J. D **59** (2010) 209.

7. Z. Tan, Y. Xia, M. Zhao, X. Liu, F. Li, B. Huang and Y. Ji, Nucl. Instrum. Methods Phys. Res. B **222** (2004) 27.

8. Z. Tan, Y. Xia, M. Zhao and X. Liu, Nucl. Instrum. Methods Phys. Res. B **266** (2008) 1938.

9. Z. Tan, Y. Xia, X. Liu, M. Zhao and L. Zhang, Appl. Radiat. Isot. **67** (2009) 625.

10. S. Tanuma, C.J. Powell and D.R. Penn, Surf. Interface Anal. **37** (2005) 978.

11. A. Jablonski, S. Tanuma and C.J. Powell, Surf. Interface Anal. **38** (2006) 76.

12. T. Nagatomi and K. Goto, Phys. Rev. B **75** (2007) 235.

13. D. Tahir, E.K. Lee, S.K. Oh, T.T. Tham, H.J. Kang, H. Jin, S. Heo, J.C. Park, J.G. Chung and J.C. Lee, Appl. Phys. Lett. **94** (2009) 212902.

14. Hajati, O. Romanyuk, J. Zemek and S. Tougaard, Phys. Rev. B **77** (2008) 1.

15. D. Tahir, E.K. Lee, S.K. Oh, H.J. Kang, S. Heo, J.G. Chung, J.C. Lee and S. Tougaard, J. Appl. Phys. **106** (2009) 084108.

16. D. Tahir, E.K. Lee, E.H. Choi, S.K. Oh, H.J. Kang, S. Heo, J.G. Chung, J.C. Lee and S. Tougaard, J. Phys. D: Appl. Phys. **43** (2010) 255301.

17. O. Romanyuk, P. Jiricek, J. Zemek, S. Tougaard and T. Paskova, J. Appl. Phys. **110** (2011) 043507.

18. D. Tahir, H.J. Kang and S. Tougaard, ITB J. Sci. **43A** (2011) 199.

19. D. Tahir, S.D.A. Ilyas and H.J. Kang, Makara Sains **15** (2011) 193.

20. D. Tahir, Y.J. Cho, S.K. Oh, H.J. Kang, H. Jin, S. Heo, J.G. Park, J.C. Lee and S. Tougaard, Surf. Interface Anal. **42** (2010) 1566.

21. D. Tahir, E.K. Lee, S.K. Oh, H.J. Kang, E.H. Lee, J.G. Chung, J.C. Lee and S. Tougaard, Surf. Interface Anal. **42** (2010) 906.

22. D. Tahir and S. Tougaard, J. Appl. Phys. **111** (2012) 054101.

23. D. Tahir and S. Tougaard, J. Phys.: Condens. Matter **24 (**2012) 175002.

24. Y.S. Denny, H.C. Shin, S. Seo, S.K. Oh, H.J. Kang, D. Tahir, S. Heo, J.G. Chung, J.C. Lee, and S. Tougaard, J. Electron. Spectrosc. Relat. Phenom **185** (2012) 18.

25. H.C. Shin, D. Tahir, S. Seo, Y.R. Denny, S.K. Oh, H.J. Kang, S. Heo, J.G. Chung, J.C. Lee and S. Tougaard, Surf. Interface Anal. **44** (2012) 623.

26. S. Tougaard and I. Chorkendorff, Phys. Rev. B **35** (1987) 6570.

27. F. Yubero and S. Tougaard, Phys. Rev. B **46** (1992) 2486.

28. F. Yubero, J.M. Sanz, B. Ramskov and S. Tougaard, Phys. Rev. B **53** (1996) 9719.

29. S. Tougaard, F. Yubero, 2008 QUEELS-ε(k,ω)-REELS: *Software Package for Quantitative Analysis of Electron Energy Loss Spectra; Dielectric Function Determined by Reflection Electron Energy Loss Spectroscopy.* Version 3.02. http://www.quases.com

30. Ashley and Anderson, J. Electron Spectrosc. **24** (1981) 127.